Experimental Study of Brittle Fracture with Plastic Strain at Cruciform Butt Joints[†]   (Report II)

—Effect of cyclic loading—

Yoshihiro SAKINO*, Hideyuki KAWAZU**, Hisaya KAMURA***
and Kohsuke HORIKAWA****

Abstract

In The Great Hanshin-Awaji Earthquake Disaster, brittle fractures with plastic strain were observed in beam-column connections of steel building frames. It is considered that the mechanical properties of weld metal, especially the ductility, affected the fractures.

In Report I, we described monotonic bi-axial loading test results using cruciform butt specimens welded by three types of welding consumable. We examined the effect of the mechanical properties of weld metal on fractures under monotonic loading.

In this Report II, we describe cyclic bi-axial loading test results using cruciform butt specimens that are the same as Report I. The purpose of this paper is to examine the effect of cyclic loading on fractures.

The main results are summarized as follows. 1) The fracture-surface appearance mainly depends on the specimen temperature, regardless of the loading pattern. But the brittle fracture-surface ratios tend to decrease in the order the magnitude of Charpy absorbed energies of the weld metal under cyclic loading. 2) Similarly, in the results under monotonic loading, it follows that the specimen that has the larger Charpy absorbed energy also has the larger elongation in the bi-axial test under cyclic loading, even if the elongation values by tensile tests are equal. 3) In the specimen with the ductile weld metal, the load declined gradually under cyclic loading, whereas all specimens fractured immediately under monotonic loading. 4) In the specimens with the brittle weld metal, they fractured suddenly and in a brittle fashion without load-down at -40°C under cyclic loading and the elongation was much smaller than that in the ductile weld metal. 5) In the specimens with the brittle weld metal, the elongation was smaller than in the ductile weld metal even at room temperature under cyclic loading.

KEY WORDS: (Damage due to Earthquake) (Steel Structures) (Welded Joints)(Cruciform Joints) (Brittle Fracture)(Bi-axial Loading) (Cyclic Loading)

1. Introduction

In The Great Hanshin-Awaji Earthquake, fractures were observed in beam-column connections of steel building frames. These parts have the largest load, so that they become the most important part of the frame. These fractures are divided into two types, either due to insufficient strength or to brittle fracture. The former type was found in comparatively older buildings welded according to the old design standards. However the latter type of damage occurred in connections welded according to the present design standards. It was ascertained by marks of local buckling, peeling of paint or mill scale and Luders's lines, that these fractured after plastic deformations. In this context, these are regarded as "general yield brittle fractures", because they fractured at stress concentration points or discontinuous points of shape after absorption of seismic energy. More studies are needed about the influencing factors and about the energy absorption capacity of general yield brittle fracture. [1)-5)]

Typical modes of brittle fracture in beam-column

connections are divided as follows.

(Mode-A) Brittle fractures in the base metal at beam-flanges, starting from the toe of the weld access hole (scallop) in the web.

(Mode-B) Brittle fractures in the base metal, heat-affected zone or weld metal of welded connections, starting from the backing strip or the end tab.

It is considered that the mechanical properties of the base metal and the detail of the scallop, the backing strip and the end tab have substantial effects on the Mode-A and Mode-B forms of fracture. It was reported that the plastic deformation-capacity of the beam to column connections became large following improvement of the detail of the scallop[6].

As well as the above influencing factors, it can be considered that the mechanical properties of the weld metal, especially the ductility of the weld metal, have substantial effects in Mode-B. (In this paper, the mechanical properties represent the absolute values of the elongation in the tensile test and the absorbed energy in Charpy impact test.) In the Report I[7], we described monotonic bi-axial loading test results using cruciform butt specimens welded by three types of welding consumable. The purpose of the Report I was to clarify the effect of the mechanical properties of weld metal on fractures under monotonic loading. The main results were summarized as follows. 1) In the case of the ductile weld metal, it presented a brittle fracture-surface at -40 °C but the elongation was equal to, or greater than, that at room temperature that presented a ductile fracture-surface. But in the case of the brittle weld metal, the elongation fell to less than 1/2 mainly because the brittle fracture occurred after the plastic deformation. 2) The fracture-surface appearance only depends on the specimen temperature and not depends on the mechanical properties of the weld metal. The elongation value in the bi-axial tests tends to become large and the fracture-surface also tends to appear ductile with rising

specimen temperature. 3) It follows that the specimens that have the larger Charpy absorbed energy have the larger elongation in the bi-axial test, even if the elongation values by tensile tests are equal.

During an earthquake, the structures endure cyclic loading. It is necessary to clarify the effect of cyclic loading. In this Report II, we describe cyclic bi-axial loading test results for cruciform butt specimens that are the same as Report I. The purpose of this paper is to examine the effect of cyclic loading and to clarify the difference between monotonic and cyclic loading on fractures.

2. Experimental Details
2.1 Shape of the specimen

The specimen for the bi-axial loading test is the same in Report I and is shown in **Fig. 1**. It is modeled on a cruciform joint by taking out the part of the beam-flange to column-flange connection. In the specimen, butt welds are at the crossover point of flanges which appear to be the most critical zone for fracture. Single bevel grooves with full penetration are used to make the cruciform butt weld. After welding, excess weld metal is removed and the width of the weld part is narrowed from 40mm to 30 mm. Moreover an artificial notch (Width: 0.2mm, Depth: 2mm) is added in the thickness direction as an initial defect by the electric wire-cut method. The detail of weld zone is shown in **Fig. 2**.

2.2 Experimental parameters

The ductility of the weld metal and temperature of the specimen are varied in this experiment.

2.2.1 Ductility of Weld metals

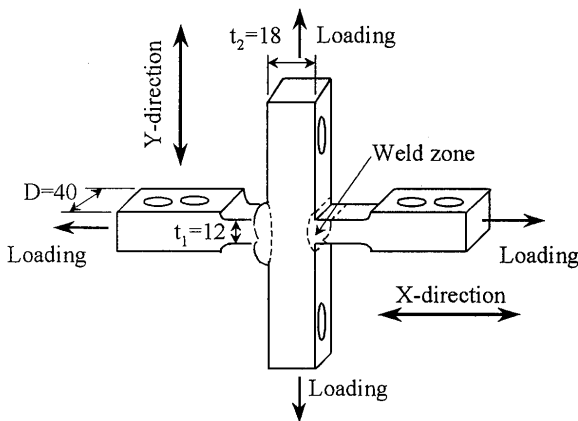Three types of weld metal are used in this experiment. The Y-series specimens are welded by CO_2
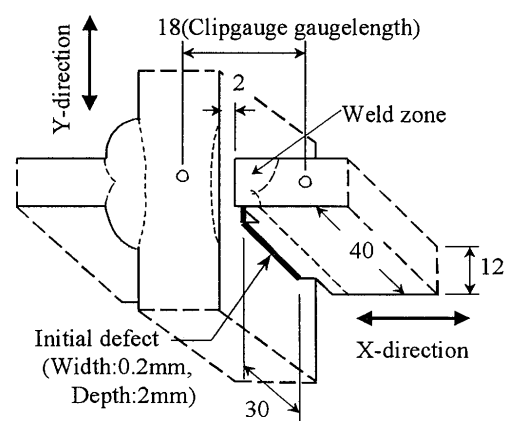

Fig.1 A conception shape of cruciform butt specimen

Fig.2 Detail of weld zone and measuring points

shielded gas wire (JIS Z 3312 YGW11), the D-series specimens are welded by covered electrode (JIS Z 3211 D4301) and the S-series specimens are welded by self-shielded wire (JIS Z 3313 YFW-S50GX). The minimum value of Charpy observed energy is provided for YGW11 and D4301 (47J at 0°C), but not provided for YFW-S50GX in JIS. (JIS: Japanese Industrial Standard)

Table 1 and **Fig. 3** show tensile test results for each weld metal. **Table 2** and **Fig. 4** – **Fig. 6** show Charpy impact test results for each weld metal. **Fig. 7** shows the comparisons of energy transition curves of all weld metals. JIS Z 2201 No.14 test pieces (diameter:10mm) were used for the tensile test and JIS Z 2202 No.4 test pieces for the Charpy impact test. All test pieces of weld metal were cut from deposited parts. Energy and fracture transition curves by Charpy impact test are fitted by the numerical formula quoted from reference [8].

In the results of tensile tests, the Y-series and the D-series show large elongation values ε_f (over 30%) whereas the S-series are lower (about 16%). Reduction of area ϕ of the S-series is also 1/3 of the Y-series. The values of yield stress σ_y and tensile strength σ_u increase in the order the S-series, the Y-series and the D-series. In each series, the value of the yield and tensile stress at -40°C becomes about 10% larger than that at room temperature.

The Charpy absorbed energies of the Y-series are over 100J, either at room temperature or -40°C. The D-series are over 100J at room temperature but equal to or less than 27J at -40°C. The S-series are less than 27J in all ranges from -40°C to +60°C and increase ratio by

rising of temperature is also small. The value of 27J is a minimum that is required for steels for welded building structures in JIS. The energy transition temperature vT_{rE} and the fracture surface transition temperature vT_{rS50} of the Y-series are about –20°C. On the other hand, the brittle fracture surface ratio of the S-series at +60℃ is about 90%, so it seems that vT_{rE} and vT_{rS50} of the S-series are very high (at least more over +60°C).

As these material test results suggest, the weld metal of the Y-series is high ductility metal (ductile weld metal), the S-series has low ductility metal (brittle weld metal) and the D-series is middle of the Y-series and S-series.

2.2.2 Temperature of specimens

It is generally known that the strain rate affects the deformation and fracture of steel. In fact, it is considered that the high strain ratio is one of the substantial causes of damage in The Great Hanshin-Awaji Earthquake. Because the fracture toughness of steel declines with
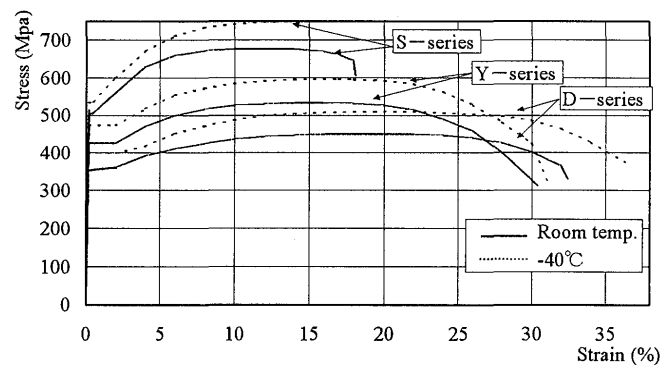

Fig.3 Stress-strain curves of weld metal by tensile test

Table1   Results of tensile test (Weld metal and Base metal)

| | Weld metal | | | | | | | | Base metal | | | | | | | |
| | -40°C | | | | Room temp. | | | | -40°C | | | | Room temp. | | | |
	σ_y (MPa)	σ_u (MPa)	ε_f (%)	ϕ (%)	σ_y (MPa)	σ_u (MPa)	ε_f (%)	ϕ (%)	σ_y (MPa)	σ_u (MPa)	ε_f (%)	ϕ (%)	σ_y (MPa)	σ_u (MPa)	ε_f (%)	ϕ (%)
Y-series	483	608	31	70	437	541	31	74	334	531	38	69	290	476	37	72
D-series	392	504	34	56	343	448	30	59	293	465	37	67	267	427	36	69
S-series	526	749	16	17	500	683	17	28	334	531	38	69	290	476	37	72

Table2   Results of Charpy impact test (Weld metal and Base metal)

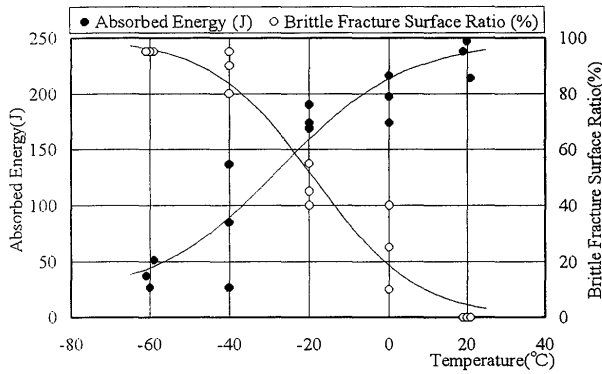| | Weld metal | | | | | | | Transition temp. (°C) | | Base metal | | | | | |
| | Absorbed energy(J) | | | | | | | | | Absorbed energy(J) | | | | | |
	-60°C	-40°C	-20°C	0°C	+20°C	+40°C	+60°C	vT_{rE}	vT_{rS50}	-80°C	-60°C	-40°C	-20°C	0°C	+20°C
Y-series	35	126	178	195	232	—	—	-27.2	-18.9	—	151	144	176	236	252
D-series	28	25	46	109	134	—	—	-8.8	-8.5	12	48	148	151	189	—
S-series	—	11	—	13	19	20	22	60<	60<	—	151	144	176	236	252

Fig.4 Energy and fracture transition curves
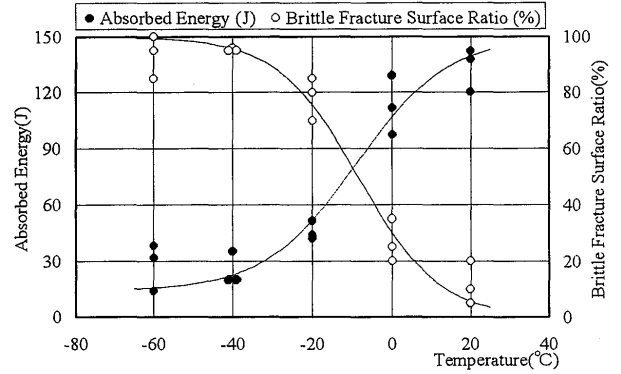by Charpy impact test (Y-series)

Fig.5 Energy and fracture transition curves
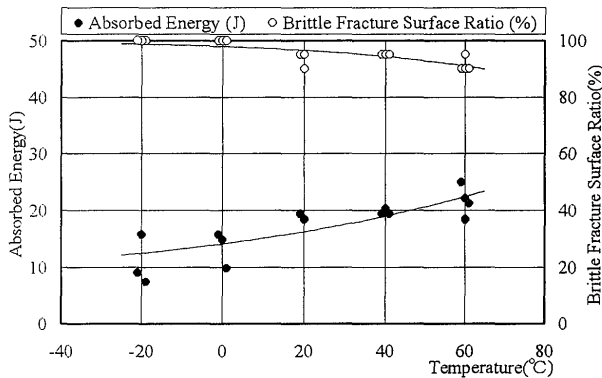by Charpy impact test (D-series)

Fig.6 Energy and fracture transition curves
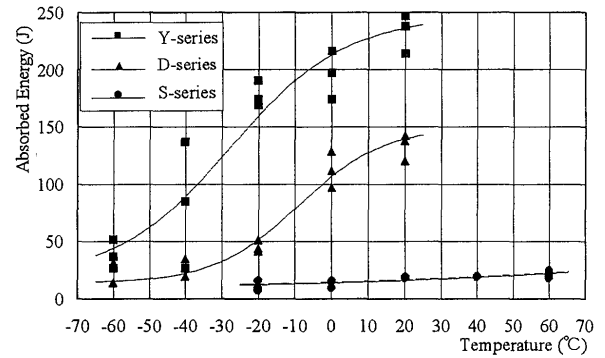by Charpy impact test (S-series)

Fig.7 Comparison of energy transition curves

raising strain rate, in the same way, fracture toughness of steel also declines with low test-temperature. As the parameter to evaluate the effect of the strain rate and low test temperature equivalently, a strain rate – temperature parameter (R) is proposed.[9)10)]

$$R = T \cdot \ln(A/\dot{\varepsilon})$$

$\dot{\varepsilon}$ = Strain rate (1/s)

A = Variable 10^8(1/s)

T = Temperature (K)

So it becomes possible to substitute for high strain rates in static tests at low temperature by using this R-parameter.

Experiments were done not only at room temperature but also -40°C. The strain rate after yield in a static test is usually from 10^{-4} to 10^{-3}/s. Experiments at strain rates from 10^{-4} to 10^{-3}/s at -40°C can be regarded as the same condition as for strain rates from 6×10^{-3} to 4×10^{-2}/s at 0°C temperature by using this R-parameter. The strain rate in The Great Hanshin-Awaji Earthquake was not measured, but by the analysis the strain rate at the beam-flange in beam-column connection is estimated from 10^{-2} to 10^{-1}/s.[11)] From the above, static experiments at -40°C can approximately represent the loading condition in The Great Hanshin-Awaji Earthquake.

During the low temperature experiments the specimens were cooled by ethyl alcohol and liquid nitrogen kept at -40±2°C. Temperatures were measured by two points of thermocouples (C-C type) fixed on the specimen.

2.3 Loading and measuring method

The Bi-axial fatigue machine was used in the experiment. This machine has four jacks and can load in two directions at the same time.

Cyclic loading pattern that was used in this experiment is shown in **Fig. 8**. First the specimen is subjected to tensile load (60% of yield strength of base metal) in the Y-direction and kept loaded, then cyclically loaded in the X-direction. It seems that this condition (stresses in Y-direction in tension) is the most severe for fracture. This stress condition corresponds to a beam-column connection subjected to the vertical vibration or the tensile force by the overturning moment during earthquake.

The displacements between the gauge-length 18mm, shown in Fig.2, were measured by two clip-gauges fixed to both sides of the specimen.
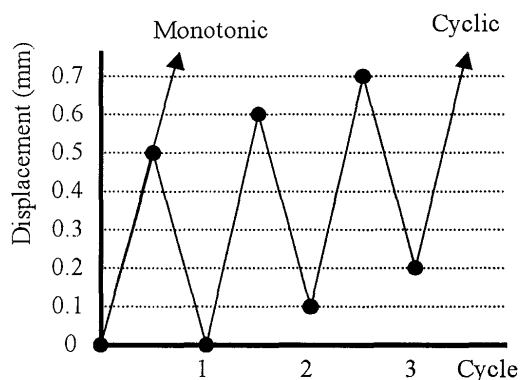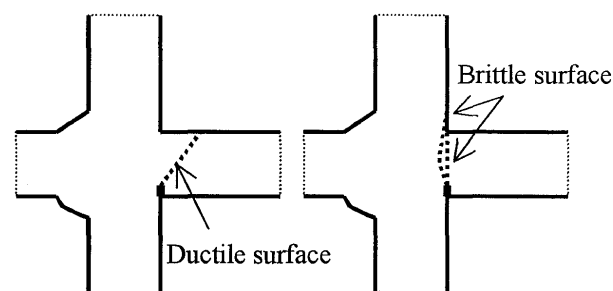
Fig.8   Cyclic pattern.

Fig .9   Fracture pattern

3. Results and Discussion

Table 3 shows the results of the bi-axial tensile test. Load-displacement relationships of the Y-series, the D-series and the S-series at the room temperature and -40°C are shown in **Fig. 10–Fig. 15**. The displacement in these figures is the average of two clip-gauge readings.

As in the case of monotonic loading, three types of fracture-surface, ductile fracture-surface, brittle fracture-surface and intermingled fracture-surface were observed. In the intermingled fracture-surface specimen, it seems that the brittle fracture occurred after developing the ductile crack (D⇒B: ductile ⇒ brittle). In Fig.10-Fig.15 and Fig.16-Fig.19, symbol ○ means the ductile fracture-surface, symbol ● means the brittle fracture-surface and symbol ◕ means the intermingled fracture-surface (D⇒B, area ratio of black in the symbol shows brittle fracture-surface ratio). **Figure 9** shows the fracture pattern of ductile fracture and brittle fracture. In the specimen with a ductile fracture-surface, the crack

runs at 45° to the Y-direction from the tip of the initial defect. But in the specimen with a brittle fracture-surface, the crack runs at right-angles to the Y-direction from the tip of the initial defect. Fig. 14 – Fig. 16 in Report I show the specimens that fractured with a ductile fracture-surface, with a brittle fracture-surface and with an intermingled fracture-surface.

3.1 Influence of the weld metal under cyclic loading

Only in the case of the S-series at -40°C, the specimen fractured suddenly and in a brittle fashion without load down after the maximum load. In the other specimens, the load at every cycle declined gradually after the maximum load shown at the 2nd –9th cycle. So in the case of D-series and S-series(at room temperature), it continuously pulled in the X-direction until it fractured after the load declined to 90% of the maximum load (it is presented as the 10% load-down in this paper). But in the case of the Y-series (except YCR-2), it continuously pulled until it fractured after the 17th

Table 3   Results of bi-axial cyclic test

Specimen No.	Temp. (°C)	Loading pattern	Max. load (kN)	Displacement of clip gauge(mm)		Fracture surface (Brittle fracture ratio)
				Max. load (cycle)	10% Down (cycle)	
YCR-1	25	Cyclic	181.16	1.01 (6)	2.1(17)*	Ductile(0%)
YCR-2	25	Cyclic	177.74	0.92 (5)	1.59 (12)	Ductile(0%)
YCL-1	-40	Cyclic	188.86	1.34 (9)	2.1(17)*	Ductile(0%)
YCL-2	-40	Cyclic	187.72	0.89 (5)	2.1(17)*	D→B(60%)
DCR-1	25	Cyclic	153.18	0.77 (4)	1.10 (7)	Ductile(0%)
DCR-2	25	Cyclic	147.85	0.71 (3)	0.80 (4)	Ductile(0%)
DCL-1	-40	Cyclic	161.03	0.79 (4)	1.56 (12)	D→B(50%)
DCL-2	-40	Cyclic	169.36	1.10 (7)	1.76 (13)	D→B(60%)
SCR-1	30	Cyclic	171.27	0.60 (2)	0.74 (3)	Ductile(0%)
SCR-2	20	Cyclic	174.07	0.79 (4)	1.10 (7)	D→B(65%)
SCL-1	-40	Cyclic	176.95	0.57 (2)	Max. load (3)	Brittle(100%)
SCL-1	-40	Cyclic	175.15	0.58 (2)	Max. load (3)	Brittle(100%)

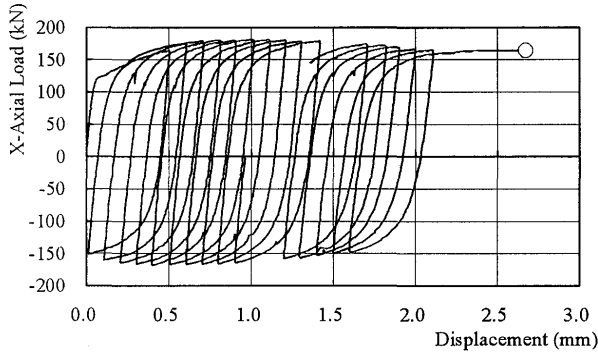*: pulled after the 17th cycle without the 10% load-down

Fig.10 X-axial load – displacement relationship
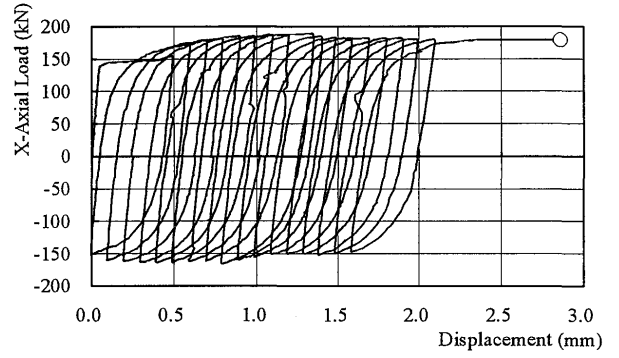*(Y-series, Room temp.)*

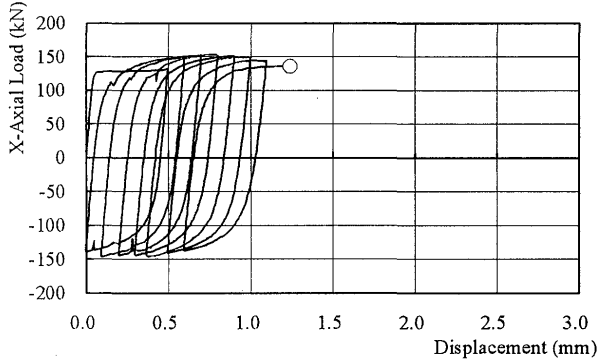**Fig.11** X-axial load – displacement relationship
(Y-series, -40°C)

Fig.12 X-axial load – displacement relationship
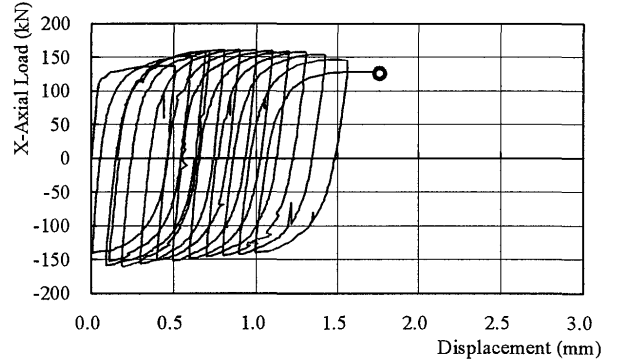*(D-series, Room temp.)*

Fig.13 X-axial load – displacement relationship
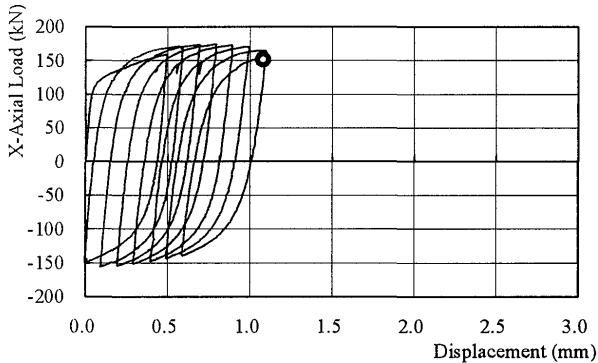*(D-series, -40°C)*

Fig.14 X-axial load – displacement relationship
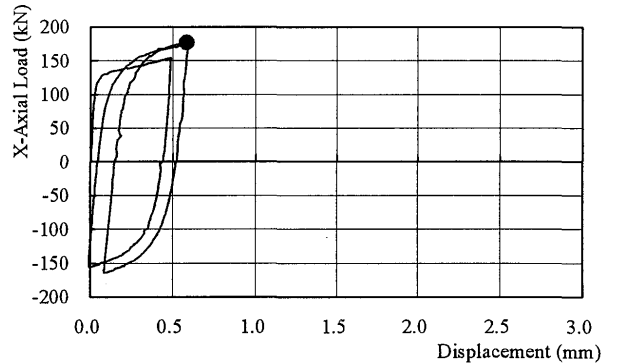*(S-series, Room temp.)*

Fig.15 X-axial load – displacement relationship
(S-series, -40°C)

cycle without the 10% load-down. Because the decline ratios of the Y-series were very small and it seemed sufficient to compare with the other series. In this paper, the elongation under cyclic loading represents the displacement at the 10% load-down. In Table 3,not only the displacement and the cycle at the maximum load, but also those at the 10% load-down are shown.

In the case of room temperature, mainly ductile fracture-surfaces appeared. On the other hand, mainly brittle fracture-surfaces appeared in the case of -40°C in all series. As for the results under monotonic loading, the fracture-surface appearance depends on the specimen temperature under cyclic loading.

The absorbed energy in Charpy impact test of the weld metal increase in the order the Y-series, the D-series and the S-series. Regardless of the loading pattern, the elongation in the bi-axial test also follows this order at room temperature and moreover at -40°C. The elongation of the S-series at -40°C is much smaller than that of the Y-series and D-series caused by the sudden brittle fracture without load-down. In the tensile test, the elongation of the Y-series and the D-series are almost the same, but in the bi-axial test the elongation of Y-series is larger than that of the D-series under cyclic loading.

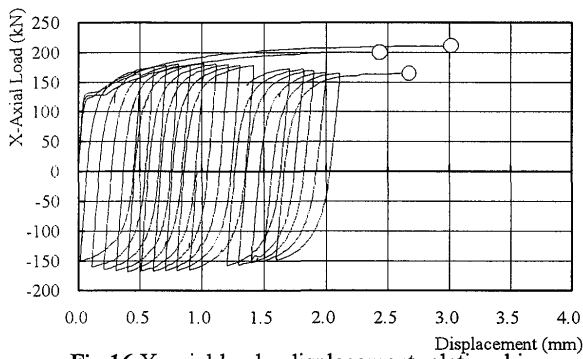Comparing with room temperature and with -40°C,

Fig.16 X-axial load – displacement relationship

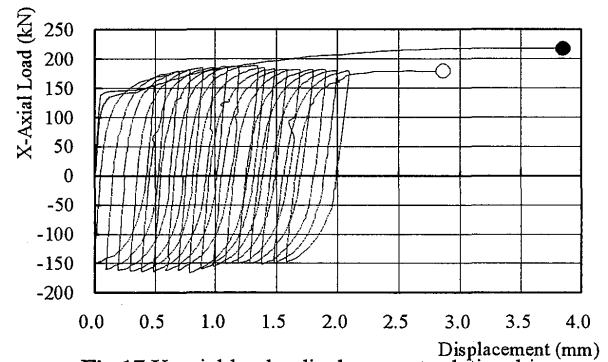*(Y-series, Room temp., Monotonic and cyclic)*

Fig.17 X-axial load – displacement relationship
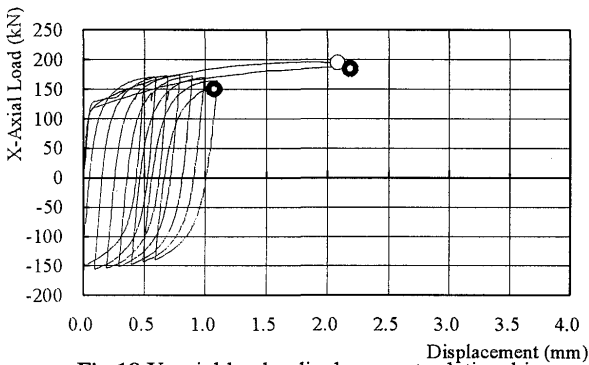
(Y-series, -40°C, Monotonic and cyclic)

Fig.18 X-axial load – displacement relationship

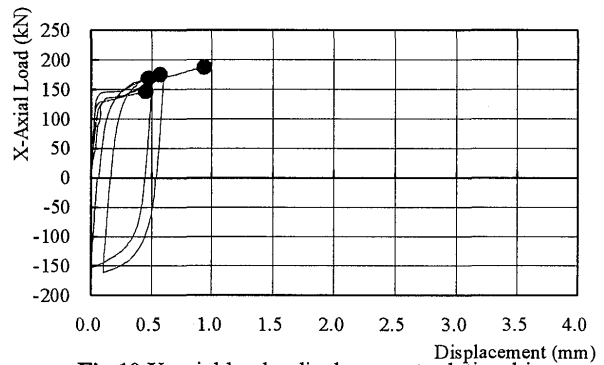*(S-series, Room temp., Monotonic and cyclic)*

Fig.19 X-axial load – displacement relationship

(S-series, -40°C, Monotonic and cyclic)

the Y-series specimens and the D-series specimens tend to have larger elongation at -40°C than that at room temperature. On the other hand, the S-series specimens at -40°C tend to have smaller elongation than at room temperature because of the sudden brittle fracture without load-down after maximum load.

3.2 Comparison with monotonic loading

In this section, the bi-axial test results under cyclic loading and monotonic loading are compared. **Fig. 16 – Fig. 19** show X-axis load-displacement relationships under cyclic loading and monotonic loading for the Y-series and the S-series.

Regardless of the loading pattern, mainly ductile fracture-surfaces appeared at room temperature and mainly the brittle fracture-surfaces appeared at -40°C. But the brittle fracture-surface ratios at -40°C decrease in the order the S-series, the D-series and the Y-series under cyclic loading. Especially in the Y-series at -40°C, the brittle fracture-surface ratios under cyclic loading are small compared with those under monotonic loading.

Except for the S-series at -40°C, the maximum load under cyclic loading is about 10% smaller than that under monotonic loading. And under cyclic loading the load at every cycle declined gradually after a maximum

load, whereas under monotonic loading all specimens fractured immediately after the maximum load. The displacement at the maximum load under cyclic loading is much smaller than that under monotonic loading. The maximum load and the displacement at maximum load of the S-series specimens at -40°C are approximately equal under cyclic loading and under monotonic loading caused by the sudden brittle fracture without load-down after maximum load.

Compared with the elongation at room temperature and at -40°C, in the Y-series the elongation at -40°C tend to be larger than that at room temperature. On the other hand, in the S-series the elongation at -40°C is much smaller than that at room temperature caused by the brittle fracture after yield. Compared with the Y-series and S-series at -40°C, the elongation of the S-series is much smaller than that of the Y-series. These observations apply to the elongation under cyclic loading and monotonic loading. But, to compare the Y-series and the S-series at room temperature, the S-series have smaller elongation than the Y-series in cyclic loading, whereas the S-series have large elongation that is approximately equal to the Y-series under monotonic loading.

4. Conclusions

In this study cruciform butt specimens that had initial defects were welded using three types of welding consumable and tested under cyclic bi-axial loading at room temperatures and -40℃. The results are compared with the results under monotonic bi-axial loading. The investigation results are summarized as follows.

(1) Mainly the ductile fracture-surfaces appeared in the case of room temperature and mainly the brittle fracture-surfaces appeared in the case of -40°C in all series under cyclic loading. The fracture-surface appearance mainly depends on the specimen temperature, regardless of the loading pattern. But the brittle fracture-surface ratios tend to decrease in the order the magnitude of Charpy absorbed energies of welding metal under cyclic loading.

(2) As in the results under monotonic loading, it follows that the specimens that has the larger Charpy absorbed energy have the larger elongation in the bi-axial test under cyclic loading, even if the elongation values by tensile tests are equal.

(3) In the case of the specimens with the ductile weld metal (which have large Charpy absorbed energy), the load declined gradually after a maximum load under cyclic loading, whereas all specimens fractured immediately after the maximum load under monotonic loading. The maximum load under cyclic loading was smaller than that under monotonic loading.

(4) In the case of the specimens with the brittle weld metal (which have small Charpy absorbed energy), it fractured suddenly and in a brittle fashion without load down at -40°C under cyclic loading, similar to the results under monotonic loading. The elongation was much smaller than in the case of the ductile weld metal.

(5) In the case of the specimens with the brittle weld metal, the elongation was smaller than in the case of the ductile weld metal even at room temperature under cyclic loading, whereas the elongation under monotonic loading was approximately equal.

As described above, include Report I , the fracture-surface appearance hardly depends on the ductility of the weld metal, but the elongation in bi-axial test depends on the ductility of the weld metal. The fracture-surface appearance tends to depend on temperature of specimen. These suggest that even if the fracture surface is brittle, the elongation is not always small. The elongation capacity is decided by the ductility of the weld metal.

Reference

1) M.TOYODA: How Steel Structures Fared in Japan's Great Earthquake, Welding Journal, American Welding Society, December (1995), pp.31-42

2) Committee on Steel Building Structures, The Kinki-Branch of The Architectural Institute of Japan (AIJ): Reconnaissance Report on Damages to Steel Building Structure Observed from the 1995 Hyogoken-Nanbu (Hanshin /Awa) Earthquake, 1995

3) Japanese Society of Steel Construction (JSSC): KOBE EARTHQUAKE DAMAGE TO STEEL MOMENT CONNECTIONS AND SUGGESTED IMPROVEMENT, JSSC Technical Report, No.39 (1997)

4) K.HORIKAWA and Y.SAKINO: Review of Damage in Welding Joints Caused by The Kobe Earthquake, Trans. of Welding Research Institute of Osaka University (JWRI), Vol.24 (1995), No.2, pp.1-10

5) K.HORIKAWA and Y.SAKINO: Damage due to Steel Structures Caused by the 1995 Kobe Earthquake, Structural Engineering International, J. Int. Ass. for Bridge and Structural Engineering (IABSE), Vol.6(1995), No.3, pp.182-183

6) Committee on Steel Building Structures, The Kinki-Branch of The Architectural Institute of Japan (AIJ): Full-Scale Test on Plastic Rotation Capacity of Steel Wide-Flange Beams Connected with Square Tube Columns, 1997 (in Japanese)

7) Y.SAKINO, K.HORIKAWA, H.KAWAZU and H. KAMURA: Experimental Study on Brittle Fractures with Plastic Strain at Cruciform Butt Joints (Report I): Trans. of JWRI , Vol.26(1997),No.2, pp81-88

8) F.NOGATA, J MASAKI: New fitting curve for Charpy Absorbed Energy and fracture toughness data of steel: J. of the Japanese Soc. for Strength and Fracture of materials, Vol.17(1982)No.2, pp1-13 (in Japanese)

9) P.E.Bennett, G.M.Sinclaer: Parameter representation of low-temperature yield behavior of body-centered cubic transition metals, Transaction of the ASME, (1966), 518-524

10) P.E.Bennett, G.M.Sinclaer: An analysis of the time and temperature dependence of the upper yield point iron, Transaction of the ASME, J. Basic Eng., 33(1961), 557.

11) Committee on Accumulated Plastic Deformation, The Japan Welding Engineering Society : Strength and fracture toughness of welding connections in steel building under cyclic large deformation (Interim Report I , II , III), 1996.7(in Japanese)